Decay of the 125 Gev Higgs boson into a pair of fermions

Term Paper of Steffen Landgraf at the University of Freiburg

28.08.2014

Contents

1 Introduction

Since the experiments at CERN at the LHC reported the discovery of a new particle of about 125 GeV in its vector-bosonic and electromagnetic decay modes, a great interest is taken in its coupling to fermions, too. The discovered particle is believed to be the Higgs boson of the Standard Mode (SM), which has several fixed attributes including decays to fermions.
This article provides an overview over the results of ATLAS and CMS on the measurement of the decay of the 125 GeV particle into two fermions. Two different decay channels are discussed: the di-bottomquark-decay and the decay into a pair of τ leptons. The results are obtained from both experiments by first triggering on specific Higgs production mechanisms, then extracting deviations of the experimentally measured (Cross Section) * (Branching Ratio) from theoretical predictions. The fraction of identified signal events over the number of expected events under the SM hypothesis, calculated from simulations, is called signal strength μ. It is a general measure of the compatibility of the experimental data with the predictions from the SM and serves as appropriate quantity to compare different measurements. The methods used to estimate contributions of background processes to the extracted signal events will be briefly discussed for every search.

1.1 Theory of SM Higgs to fermion decays

The SM Higgs particle is a concept to explain how elementary particles aquire their masses through couplings to the Higgs field. The coupling of the Higgs field to any massive particle X is thus given by [1]:

$$g_X = \frac{m_X}{\nu},$$

where ν ($\approx$ 246GeV) is the vacuum expectation value of the Higgs field and a parameter of the SM. This feature is the reason why the production/decays of the Higgs particle from/to the first quark and lepton generations are unfavoured compared to the generations with higher masses.
The mechanism of coupling of the Higgs field to the fermion fields is called Yukawa coupling and is the favoured theoretical approach, using the interaction Lagrangian:

$$\mathcal{L}_{\mathbf{Yukawa}}(\phi, \psi) = -g\bar{\psi}\phi\psi$$

Figure 1: Interaction Lagrangian of the Yukawa theory [2]

where ϕ stands for the real and scalar Higgs potential and ψ is a fermion's Dirac spinor. Spin 0 and the neutrality of the Higgs boson are both prerequisites of the SM Higgs boson and correspond to the properties of the field beeing scalar and real. Therefore, and due to conservation laws, it can only decay into two opposite charged fermions with opposite spin. The antifermion has the positive charge sign and can be identified with $\bar{\psi}/\bar{f}$ in the formula. The corresponding 0-th order Feynman diagram for the Yukawa coupling is:

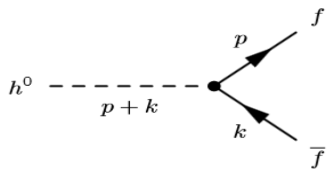

Figure 2: 0-th (perturbative) order Feynman diagram for the Yukawa coupling of the Higgs field to fermion fields [3]

To measure the coupling strengths of the Higgs particle to fermions in comparison to the SM expectations, coupling modifiers κ_F are introduced. The square of these coupling modifiers scale the observed CS*BR for a coupling process to the SM expectation value

$$\kappa_F^2 = \frac{(\sigma * BR)[measured]}{(\sigma * BR)[SM]},$$

and are expected to be consistent with 1 for a measurement matching the SM predictions. The whole measured CS*BR can be decomposed in terms of an SM coupling CS*BR and deviations described by the coupling modifiers:

$$\sigma \cdot BR(ii \rightarrow H \rightarrow ff) = \sigma_{SM} \cdot BR_{SM} \frac{\kappa_i^2 \cdot \kappa_f^2}{\kappa_H^2}$$

Figure 3: Dependence of the measured CS*BR on the CS*BR of the SM with coupling modifiers κ, accounting for discrepancies [4]

The spin information is ignored in the measurements, because it is not possible to keep track of it in the decay products. Yet, the requirement of opposite signs of the charged decay products is used as discriminating quantity.

1.2 The SM Higgs production and measurable quantities

Before looking at the decay processes of the 125 GeV Higgs boson its production processes have to be investigated, which has already been done using the vector-bosonic and electromagnetic decay modes. In the measurement of fermionic decays the fundamental selection criteria for signal events require to have a detector signature, equal to one of the main three production processes for Higgs bosons in proton collisions at the LHC.

These are gluon fusion (ggF), vector boson fusion (VBF) and vector boson associated production (VB), shown as Feynman graphs here:

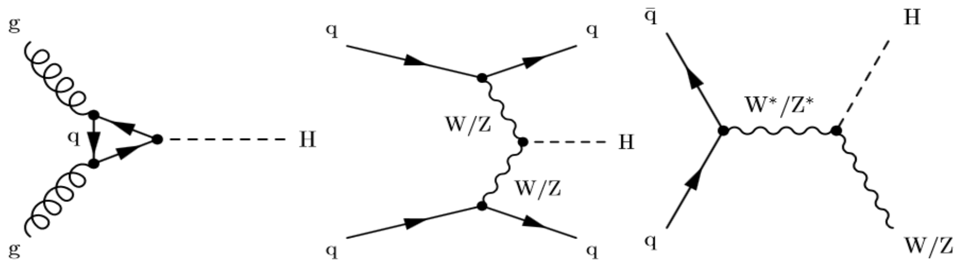

Figure 4: Most probable Higgs production processes in LHC pp collisions: gluon fusion (left), vector boson fusion (middle), vector boson associated production (right)[5]

The processes can be distinguished, because each of them has characteristical features. While there are two light jets close to the beam axis in the VBF production mode, it is more likely to have higher p_T of the generated Higgs boson (coming from ISR of gluons) in case of the gluon fusion process. The VB associated production process requires the previous production of a W/Z boson with a high mass.

At $\sqrt{s} = 8TeV$ $(/7TeV)$, the energy at which the data for the searches was taken, the most probable Higgs production process is the gluon fusion (see Fig.5). All of the cross sections in the different production modes rise with increasing energy.

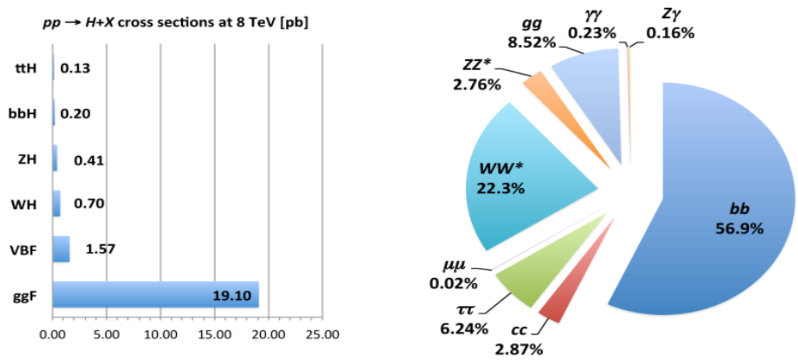

Figure 5: Higgs production cross sections at $\sqrt{s} = 8TeV$ in pb (left) and branching ratios (right)[6]

The plot of branching ratios (right) shows how the coupling of the Higgs particle to other particles with larger masses is enhanced. The decay to a pair of top quarks, as heaviest

of all known elementary particles, is kinematically not allowed and does not contribute at all. For this reason, more than every other of the produced Higgs particles decays into a pair of bottom quarks. The branching ratio for the decay into the lighter τ leptons is much lower and about 6% but is by far the largest one of the decays into leptons.
The reason for the low branching ratios for vector bosons - compared to their high masses - is given by the need of one of them beeing virtual (to sum up to the Higgs mass). The decay is then kinematically possible but occurs with a lower rate

2 Measurements

Measurements on both decay modes based on different techniques were performed independently at the ATLAS and CMS experiment. The processing of data of the two experiments is set up indepently in order to obtain non correlated measurements. After an introduction to the general features of a specific decay mode, the different searches are discussed separately for each decay mode (τ/b-quark decay). The different methods of ATLAS and CMS to analyze data are compared with regard to their main aspects as well as their results.

2.1 The search for the SM Higgs decaying to a pair of bottom quarks

The decay of the Higgs particle into a pair of bottom quarks cannot be investigated in inclusive searches, due to huge multijet-, diboson- and top process backgrounds. The vector boson associated production mechanism of a Higgs particle is therefore preselected and used to massively reduce background contributions. This is done by triggering on the leptonic decay of the associated vector boson by using lepton and E_T^{miss} triggers. The preselected production events then have to be accompanied by two b-quarks from the Higgs decay to count as signal event. Their reconstructed invariant jet masses are used to distinguish signal events from background contributions which arise from the decays of other vector bosons, such as $Z \rightarrow b\bar{b}$. The ATLAS and CMS experiment use different methods to correct for deviations of the measured invariant jet mass, which will be discussed separately.

The following event display shows the signature of a candidate for the process $WH \rightarrow l\nu + b\bar{b}$ in the ATLAS detector.

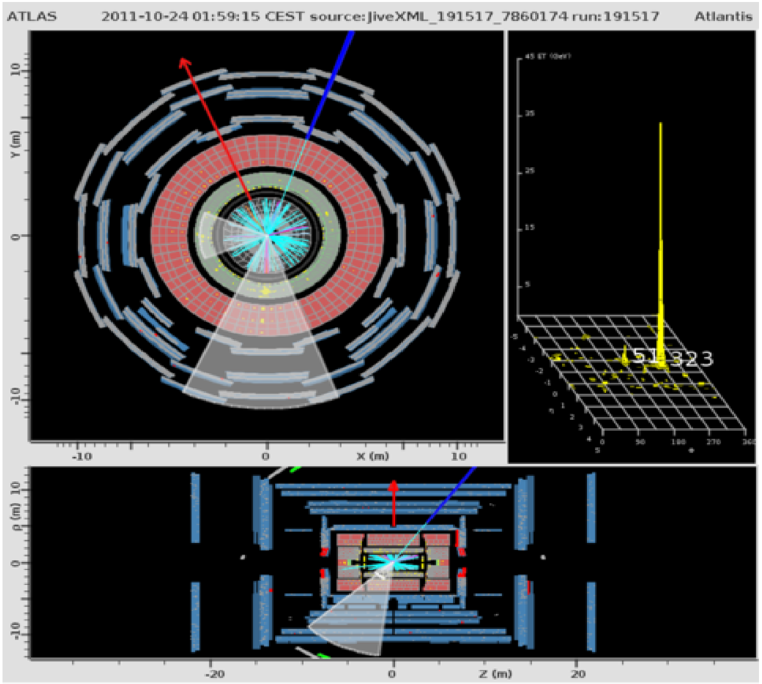

Figure 6: Event display from the ATLAS detector of a $WH \to l\nu + b\bar{b}$ candidate [7]

The red arrow corresponds to missing transverse energy from the not detectable neutrino of the W boson decay, while the blue line stands for the detected corresponding lepton. The two b-jets can be seen as energy deposition in the hadronic calorimeters, which show two sharp (yellow) peaks in the $\eta - \phi$-plane.
The main background processes to the decay $H \to b\bar{b}$ are single top and top pair production, diboson production, as well as W+jets and multijet events. These processes or even a detected part of it can be misidentified as signal event, what is seen from the final state signatures of the following Feynman graphs.

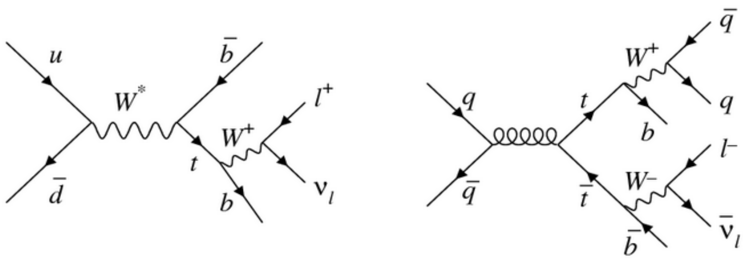

Figure 7: Single top (left) and top pair (right) production in pp-collisions [8]

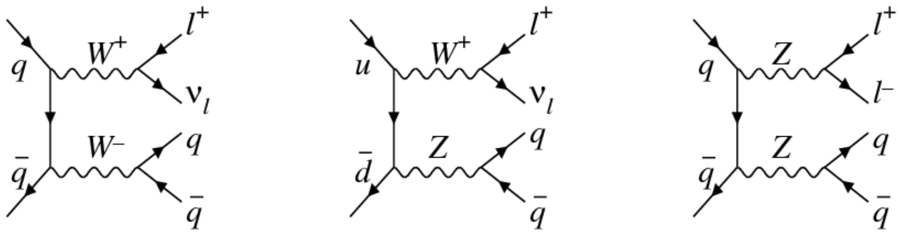

Figure 8: Diboson background processes in pp collisions for the vector boson associated Higgs production mechanism [8]

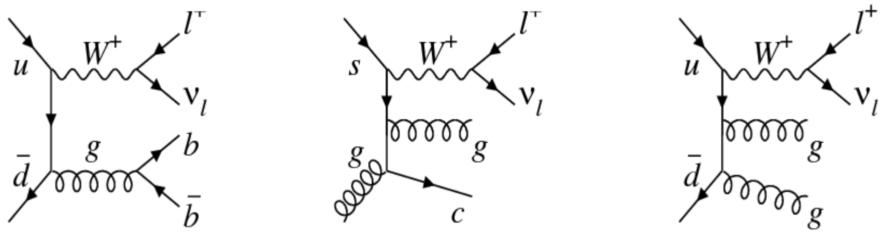

Figure 9: W+jets background processes [8]

Multijet background to the signal processes occurs if W boson production (identified by its leptonic decay, Fig.9) is accompanied by gluons or (light) quarks.

2.1.1 The ATLAS measurement of the decay of the 125 GeV Higgs boson into a pair of bottom quarks [9]

The ATLAS search for the decay of the Higgs particle into two bottom quarks uses data sets of 4.7 and 13.0 fb^{-1} recorded at $\sqrt{s}$ = 7 TeV and 8 TeV, respectively. An identification of vector boson associated Higgs production is used to extract a sample with suppressed mutijet background. This is performed by triggering on the leptonic decay modes of the associated vector boson with zero, one or two measured charged leptons, by using highly effective lepton and E_T^{miss} triggers to select the events $Z \to \nu\nu$, $W \to l\nu$ and $Z \to ll$, respectively. For this purpose the track infomation of a lepton from the inner detector (if existing) is matched to the corresponding track in the outer electromagnetic calorimeter (for e) or muon chamber (for μ). The reconstructed leptons are then categorized, according to the accuracy of their identification, as tight or loose. The basic event selection criteria for the event preselection are summarized in the following table:

Table 1: The basic event selection for the three channels.

Object	0-lepton	1-lepton	2-lepton
Leptons	0 loose leptons	1 tight lepton + 0 loose leptons	1 medium lepton + 1 loose lepton
Jets	2 b-tags $p_{\mathrm{T}}^{\mathrm{jet}_1} > 45$ GeV $p_{\mathrm{T}}^{\mathrm{jet}_2} > 20$ GeV $+ \leq 1$ extra jets		
Missing E_T	$E_{\mathrm{T}}^{\mathrm{miss}} > 120$ GeV $p_{\mathrm{T}}^{\mathrm{miss}} > 30$ GeV $\Delta\phi(\boldsymbol{E}_{\mathbf{T}}^{\mathbf{miss}}, \boldsymbol{p}_{\mathbf{T}}^{\mathbf{miss}}) < \pi/2$ $\min[\Delta\phi(\boldsymbol{E}_{\mathbf{T}}^{\mathbf{miss}}, \mathrm{jet})] > 1.5$ $\Delta\phi(\boldsymbol{E}_{\mathbf{T}}^{\mathbf{miss}}, b\bar{b}) > 2.8$	$E_{\mathrm{T}}^{\mathrm{miss}} > 25$ Gev	$E_{\mathrm{T}}^{\mathrm{miss}} < 60$ GeV
Vector Boson	-	$m_{\mathrm{T}}^{W} < 120$ GeV	$83 < m_{\ell\ell} < 99$ GeV

Figure 10: Basic event selection criteria for the three channels of the Higgs production process [9]

As jet reconstruction algorithm an anti-k_t algorithm is used with a distance parameter of R= 0.4. The jet energies are corrected for the contribution from pile-up using correction factors determined from Monte-Carlo (MC) simulations. These correct the invariant dijet masses not only for their deposited energy in the hadronic and electromagnetic calorimeters, but also take into account the energy from muons produced in the jet (μ-correction). In addition, there is an energy correction which is dependent on the reconstructed kinematical properties (i.e. p_T) of the associated vector boson.
The gain in resolution on the invariant dijet mass of the two b-quarks is demonstated on an MC-simulated sample of $ZH \to ll\ b\bar{b}$ decays. The black line correponds to the dijet mass distribution before, and the red line after applying the μ- and p_T^{reco} corrections.

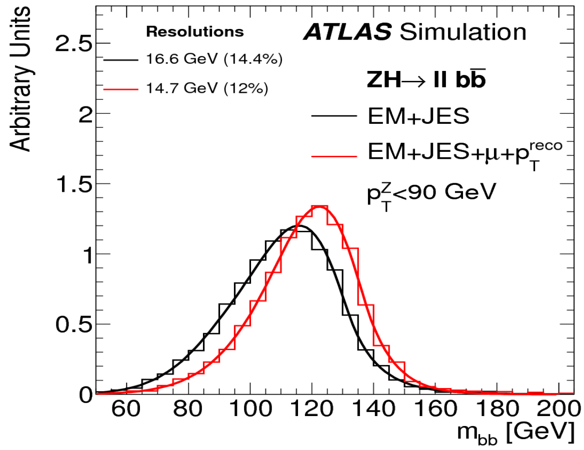

Figure 11: Basic event selection criteria for the three channels of the Higgs production process [9]

The MV 1 b-tagging algorithm is used to identify the b-quarks originating from the subsequent decay of the Higgs particle. Its efficiency for b-quark identification is 70% and it has rejection factors of 5 for c-quarks and 150 for light quarks. After the identification of the b-quarks, their mass is then used as discriminating variable for the signal extraction. As example for the treatment of the background processes the top pair production is discussed in the following. The corrresponding Feynman diagram for the $q\bar{q}$ production mode is:

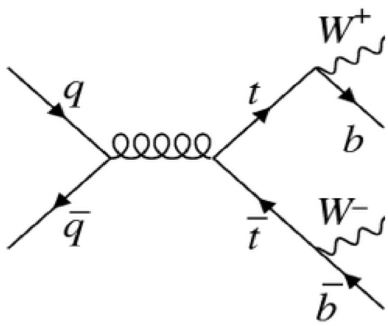

Figure 12: Top pair production with subsequent decays into W boson in pp-collisions [8]

The most probable top pair production process would be in fact from gluons, since most of the energy in 7/8 TeV pp-collisions is carried by gluons in the initial state. However, top pair processes contribute in the 1 lepton, 2 tags, 3 jets category, when one of the W bosons decays hadronically to light quarks and one of them is identified as light jet.

On the other hand there is a small contribution from signal events (due to detector acceptances or misidentification) in this category which is the reason for taking it as control region. In many control regions of the entire analysis the contributions of all background processes are simulated with MC generators at up to NNLO (Next-to Next-to Leading Order). The simultaneous fit of the simulations to the measured data in the control regions then yields scale factors. These describe the ratios of the observed background event rate over the expected background and are determined separately for the different processes.
Applying these scale factors to MC simulations in the signal region ensures a proper background estimation for signal events. Once this is done, the signal from the Higgs decay is extracted as excess of data over the background. The corresponding signal strength is the number of observed signal events over the expected one, calculated from MC simulation.

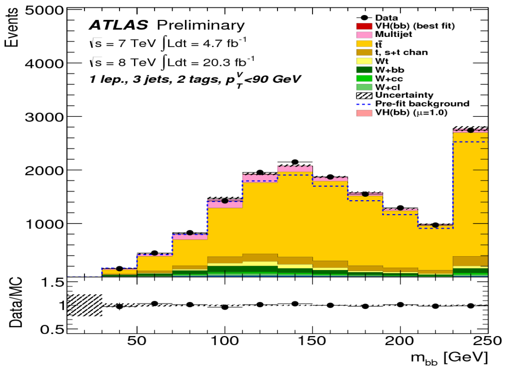

(a) $t\bar{t}$ dominated 1lep, 3 jets, 2 tags conrol region

Process	Scale factor
tt	1.13 ± 0.05
Wb	0.89 ± 0.15
Wcl	1.05 ± 0.14
Zb	1.30 ± 0.07
Zcl	0.89 ± 0.48

(b) scale factors to different background processes

Figure 13: Scale factors for MC simulated background (b), determined from control regions, e.g.:(a)[9]

To validate the analysis, a fit of the data in the same final states containing the signal strength of the process $Z \to b\bar{b}$ as additional free parameter μ_{VZ} is performed, using the same event selection. The resulting correlation between μ (the signal strength of the $H \to b\bar{b}$ process) and μ_{VZ} (the signal strength of the process $Z \to b\bar{b}$) is only 2 %, so one can trust the results of the fit of the single signal strength μ. The corresponging results for the measured signal strenths are $\mu = 0.2 \pm 0.5(stat.) \pm 0.4(sys.)$ for $H \to b\bar{b}$ and $\mu_{VZ} = 0.9 \pm 0.2$ for $Z \to b\bar{b}$.

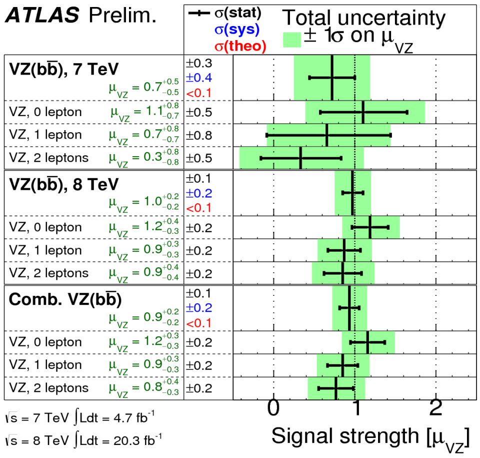

(a) measured signal strengths for VZ processes

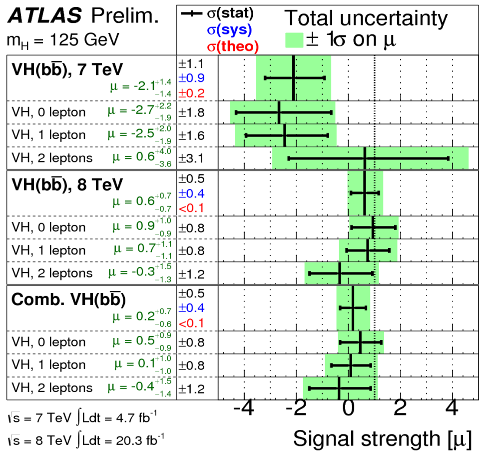

(b) measured signal strengths fo VH processes

Figure 14: ATLAS results for the measured signal strengths [9]

As shown in Fig.14(a), the measured signal strengths for all channels in the VZ processes are consistent with 1 within their errors, affirming SM predictions. The signal strengths for all VH processes in Fig.14(b) are measured to be consistent with 0, but considerable statistical and systematical errors prevent to exclude the SM hypothesis of $\mu = 1$ at a high confidence level.

2.1.2 The CMS measurement of the decay of the 125 GeV Higgs boson into a pair of bottom quarks [10]

The CMS analysis uses up to 5.1 and 18.9 fb^{-1} at $\sqrt{s} = 7$ TeV and 8 TeV, respectively. $W \to l\nu$ decays from the vector boson associated Higgs production mechanism are again used to trigger on Higgs decays. In case of $W \to \tau\nu_\tau$, only the 8TeV data set is analyzed and only 1-prong hadronic decays of the τ lepton are considered. The leptonically decaying τ particles contribute to $W \to e\nu_e$ and $W \to \mu\nu_\mu$ and are included in the analysis.
To identify the b-quarks, a combined secondary vertex b-tagging algorithm with $CSV > 0.898$ is used as discriminating value. Depending on this threshold, the b-tag efficiency is in the range of $50 - 75\%$, $5 - 25\%$ and $0.15 - 3.0\%$ for b-quarks, c-quarks and light quarks or gluons, respectively. The general method of reconstructing jets is to use an anti-k_t clustering algorithm with a distance parameter of 0.5.
To improve the precision in the reconstruction of the invariant mass of the two b-jets, an additional correction algorithm is used. It individually recalibrates an identified b-jet to the true b-quark energy. With a BDT (Boosted Decision Tree) the detailed jet structure information is taken into account, including information on the secondary vertex, tracks and jet constituents. The BDT is trained on simulated samples of $H \to b\bar{b}$ decays for this purpose. The following plot shows the dijet invariant mass distribution for simulated

$H \to b\bar{b}$ samples before (red) and after (blue) the BDT regression. The gain in resolution σ on the reconstructed invariant mass shows the improvement of invariant dijet mass resolution in the analysis.

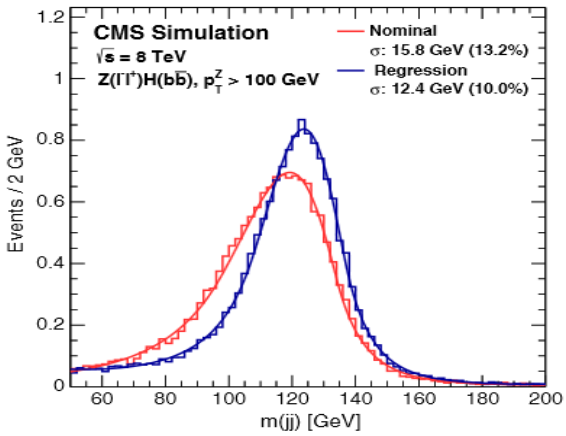

Figure 15: Dijet invariant mass for $H \to b\bar{b}$ simulated samples before (red) and after (blue) the BDT regression [10]

The BDT algorithm itself contains many decision trees, classifying the event as belonging to specific phase space regions. Each region corresponds to a specific purity of signal, because signal events occur within different parts of the phase space with different probabilities. This procedure can be done with slightly different decision trees, splitting the phase space in various ways. The boosting of the decision tree occurs, when the information of different trees is collected and superposed to form one discriminating quantity: the BDT discriminant. This discriminant is then an overall measure for the signal-likeness of an event.
The BDT is also used to calibrate the modeling of background processes in the signal regions. The scale factors, which correct the simulated event yields to the measured - are determined from control regions, i.e. W/Z+jets or top-pair production dominated regions. As example, the following table in Fig.16 shows the scale factors (for low-p_T vector bosons) for different channels of the analysis.

Process	$W(\ell\nu)H$	$Z(\ell\ell)H$	$Z(\nu\nu)H$
Low $p_T(V)$			
$W + udscg$	$1.03 \pm 0.01 \pm 0.05$	$\cdots$	$0.83 \pm 0.02 \pm 0.04$
$W + b$	$2.22 \pm 0.25 \pm 0.20$	$\cdots$	$2.30 \pm 0.21 \pm 0.11$
$W + b\bar{b}$	$1.58 \pm 0.26 \pm 0.24$	$\cdots$	$0.85 \pm 0.24 \pm 0.14$
$Z + udscg$	$\cdots$	$1.11 \pm 0.04 \pm 0.06$	$1.24 \pm 0.03 \pm 0.09$
$Z + b$	$\cdots$	$1.59 \pm 0.07 \pm 0.08$	$2.06 \pm 0.06 \pm 0.09$
$Z + b\bar{b}$	$\cdots$	$0.98 \pm 0.10 \pm 0.08$	$1.25 \pm 0.05 \pm 0.11$
$t\bar{t}$	$1.03 \pm 0.01 \pm 0.04$	$1.10 \pm 0.05 \pm 0.06$	$1.01 \pm 0.02 \pm 0.04$

Figure 16: CMS scale factors at 8 TeV for the event yields in different signal regions in the low-p_t-range of the associated vector boson derived from control regions; the first quoted uncertainty is statistical and the second is systematic [10]

These scale factors are able to accout not only for cross section discrepancies but also for residual differences in the physical event selection.
As example for a control region, Fig.17 shows the distribution in the dijet transverse momentum p_T in the Z(e^+e^-)H channel of the Z+jets control region after the scale factors where applied.

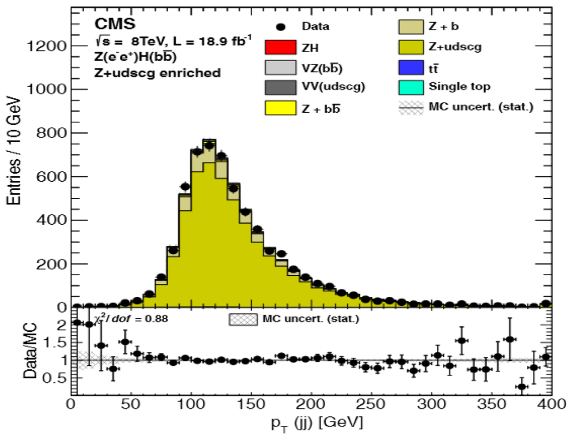

Figure 17: dijet transverse momentum ($p_T(jj)$) distribution of the Z+jets control region in the Z(e^+e^-)H channel; the bottom inset shows the observed event yields over those expected from the SM [10]

A total of 14 BDT distributions is considered, as the example in Fig.18(a), which shows the VH enriched BDT region of the high-boost events of the Z($\nu\nu$)H channel. They are combined to Fig.18(b) by gathering bins of similar expected signal-to background ratio, as given by the value of the output of their corresponding BDT discriminant.

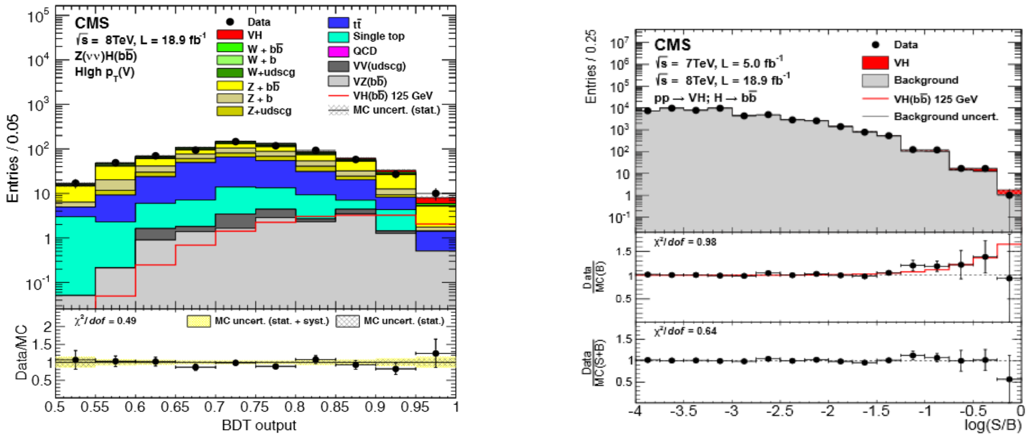

(a) VH enriched BDT region (BDT score > 0.5) of the high-boost events in the Z($\nu\nu$)H channel

(b) Combination of all channels with respect to the expected signal to background ratio

Figure 18: BDT output distributions for one specific channel (a) and all 14 channels combined (b); the bottom insets show the number of signal events over the expected value under the assumption of only measuring background or background plus signal [10]

There is an excess of data over the only-background hypothesis (dominating at high BDT scores) which is consistent with SM expectations within the error bars. The measured signal strengths for each event category as well as the combined value come out to be consistent with the SM expectation, which is visualized in Fig.19.

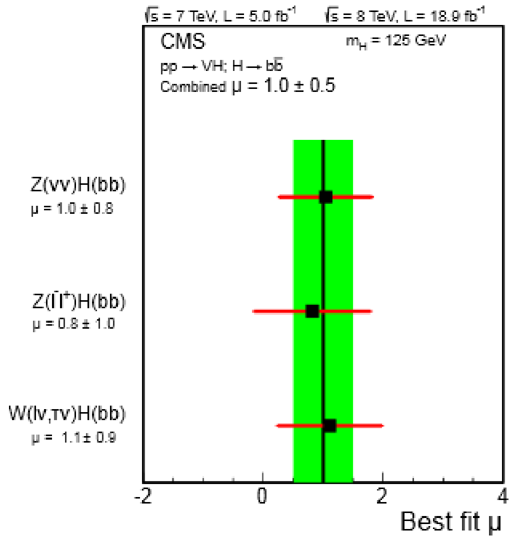

Figure 19: Measured signal strengths for the different channels with respect to the SM expecation and combined value (black line) with $\pm 1\sigma$ error interval (green bands)[10]

2.2 The measurement of the decay of the 125 GeV Higgs boson into a pair of τ leptons

The $H \rightarrow \tau^+\tau^-$ decay is - with a branching ratio of $\approx$6.2% (see: Fig.5) - among the leading decay modes for a Higgs boson of $m_H = 125$ GeV. Therefore it provides a convenient way to measure the coupling of the Higgs boson to fermions, especially as it can be tested in all three Higgs production modes, in gluon fusion, vector boson associated production and vector boson fusion.
The decay into $\tau\tau$ has a smaller contribution from background compared to the $b\bar{b}$ decay mode of the Higgs particle and a large event rate expected in the SM, in comparison to other leptonic decays.
A produced τ particle itself decays either leptonically into $\mu\nu_\mu$ or $e\nu_e$, or hadronically into one or many charged and neutral pions, under the emission of a ν_τ. Fig.20(a) shows the branching ratios for a single τ decay and Fig20(b) for a pair of τ leptons. In the following two sections, the notation τ_l / τ_h or τ_{lep} / τ_{had} refers to the leptonic / hadronic decay of a τ particle.

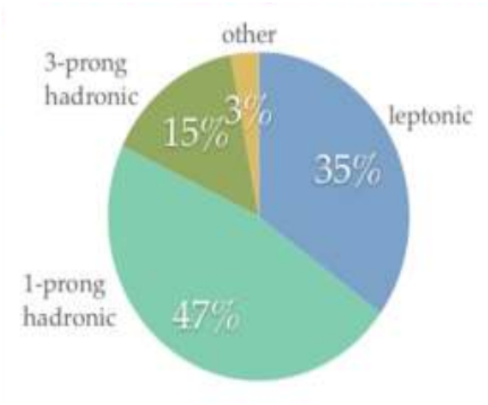

(a) τ decay branching ratios

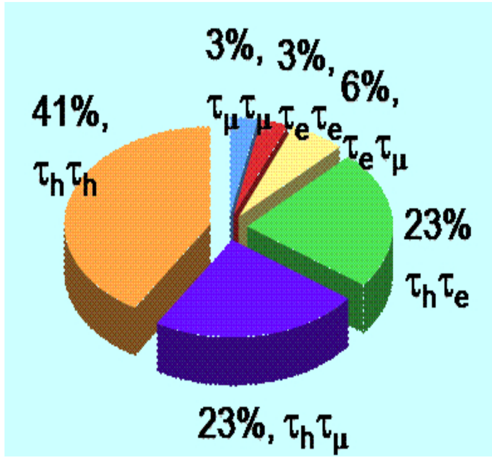

(b) Branching ratios for the decay of a τ-pair: $\tau_h \leftrightarrow$ hadronic decay , $\tau_{e/\mu} \leftrightarrow$ decay into $e\nu_e$ / $\mu\nu_\mu$

Figure 20: Branching ratios of a τ particle (left) and of a pair of τ particles (right)[6]

The aim of the searches is the identification of a τ-pair final state from a Higgs boson decay. In the analysis of both ATLAS and CMS, the first step is the reconstruction of a τ pair while the second is to further characterize the $H \rightarrow \tau\tau$ candidates according to their Higgs production mechanism. This is done by the requirement, that $H \rightarrow \tau\tau$ decays from vector boson fusion or gluon fusion only produce two charged leptons, while the vector boson associated production mode leads to one additional lepton, which arises from the decay of the associated vector boson.
All Higgs production mechanisms can give rise to jet signatures, which are dominant in the case of vector boson fusion. In this case, two high-energy jets with a large pseudo-rapidity separation are produced from the remains of the two colliding protons. This and other features of the Higgs production processes are used to distinguish them in the analysis.

2.2.1 The ATLAS measurement of the decay of the 125 GeV Higgs boson into a pair of τ leptons [11]

The ATLAS search of the decay $H \rightarrow \tau\tau$ uses data samples of proton-proton collisions of $L = 20.3$ fb^{-1} at a centre-of-mass energy of $\sqrt{s} = 8$ TeV. Following the preselection of events concerning the τ-pair decay modes in association with a specific Higgs production mechanism, data is analyzed using a BDT. This uses a set of kinematical variables to distinguish the signal-like events from background after being trained on simulated samples of events to reach maximum separation power.

To first identify the τ particles which decay leptonically, lighter leptons and E_T^{miss} from its corresponding neutrino are measured. In case of electrons/muons the information from inner tracking detectors combined with EM calorimeter responses (in case of e) or MS-tracks (for μ) is used. After the selection cuts, the probability of identifying an electron or muon by this method is $80-90\%$ and 90%, respectively.
Jets are generally reconstructed by the anti-k_t algorithm with a distance parameter of $R = 0.4$, and a jet-vertex-fraction (JVF) requirement of JVF>0.5 is used to reduce the number of selected jets of one event due to pile-up. As for other particles, the detector has a specific acceptance for the detection of jets.
Hadronically decaying τ particle reconstruction starts from clusters in the electromagnetic and hadronic calorimeters. A cone of $\Delta R < 0.2$ around the barycenter defines tracks, which are associated with the decay of the candidate for τ_h. The candidate has to fulfill the criterium of having charge ± 1 and one or 3 candidates for (prong) tracks. If there are different objects selected by this procedure which overlap within $\Delta R < 0.2$ only one is considered.
The presence of missing transverse momentum E_T^{miss} is an other important feature due to the neutrinos from τ decays. E_T^{miss} is reconstructed from calorimeter cells with the associated track from identified electrons, photons, hadronically decaying τ leptons, jets and muons.
As soon as two τ tracks associated with one vertex are found, the invariant $\tau\tau$ mass ($m_{\tau\tau}^{MMC}$) is reconstructed using the missing mass calculator (MMC). It is built to reconstruct the invariant $\tau\tau$ mass while taking into account the energy E_T^{miss} from the undetectable neutrinos, some information about decay vertices and considering the visible mass of both τ candidates. The following plot in Fig.21 shows the separation power of the MMC reconstructed mass for $Z \to \tau\tau$ and $H \to \tau\tau$ events.

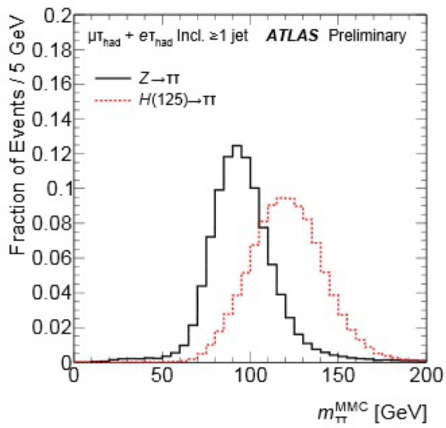

Figure 21: MMC reconstructed invariant mass of a τ pair [11]

There are different methods used for the the background estimation in the different de-

cay channels of the τ pair: For one or both of the τ particles decaying leptonically there is a background from misidentified leptons, which accounts for multijet, W+jets and semileptonic $t\bar{t}$ processes. It is estimated with the data-driven "fake-factor" method.
The irreducible background from the process $Z \to \tau^+\tau^-$ is estimated using a τ-embedded $Z \to \mu^+\mu^-$ data sample and is normalized in the final fit independently for the $\tau_h\tau_h$, $\tau_h\tau_{lep}$ and $\tau_{lep}\tau_{lep}$ channels.
Drell-Yan backgrounds from $Z/\gamma* \to e^+e^-, \mu^+\mu^-$ are simulated with the ALPGEN MC simulation and validated in control regions, for example the Z mass control region 80 GeV $< m_{\tau\tau}^{vis} <$ 100 GeV fo the $\tau_{lep}\tau_{lep}$ channel.
Top quark background processes from $t\bar{t}$ or single-top production are simulated using MC simulation and are normalized in control regions, built by inverting the b-jet veto from the signal selection.
Background contributions from diboson processes like W^+W^- are estimated from MC simulation while for W+jets processes a combination of MC and data driven methods was chosen.
It is also important to take into accout the $H \to W^+W^-$ process because it has a non-negligible contribution to the $\tau_{lep}\tau_{lep}$ channel. This process is purely MC simulated for $m_H = 125$ GeV.

To validate the MC simulations of the background models there are different control regions defined for each channel of the analysis. This is done because the composition of background processes differs between the channels. For example, the top quark control region for the $\tau_{lep}\tau_{lep}$ channel can be mentioned. It is defined by inverting the b-jet veto and gives - in this specific case - rise to an additional correction of $\Delta\phi_{ll}$ (difference in ϕ of the two lepton tracks). After this correction, the top process background in the control region for both, the VBF and Boosted (gluon fusion / VB associated production) categories, is well described by simulations.

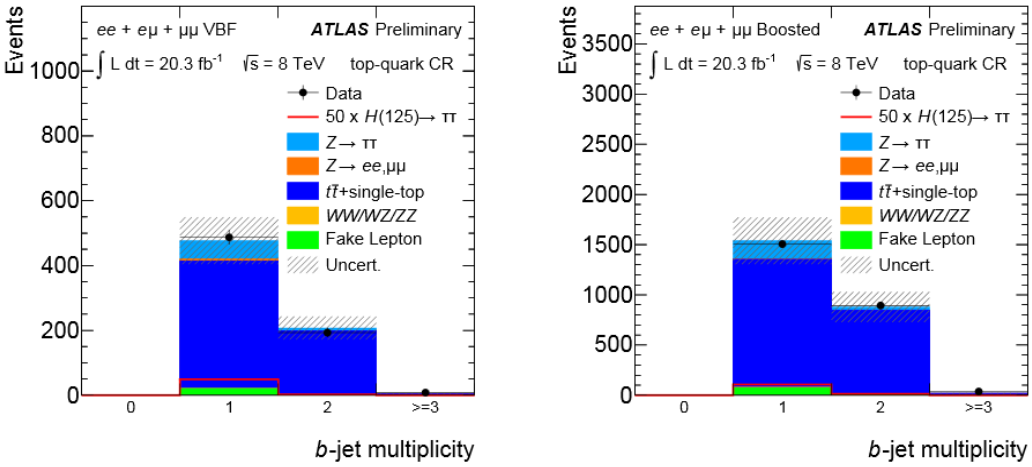

Figure 22: Jet-multiplicities after $\Delta\phi$ correction and inversion of the b-jet veto for the VBF (left) and the Boosted (right) category of the $\tau_{lep}\tau_{lep}$ channel [11]

Fig.23(a) and (b) show the results for the measured signal strengths over the SM expectations for the process $H \rightarrow \tau\tau$ for each of the three signal event categories and for all of them combined. Fig.22(b) visualizes the results as likelihood plot. The overall signal strength for the process $H \rightarrow \tau\tau$ is measured to be $\mu = 1.43^{+0.31}_{-0.29}(stat.)^{+0.41}_{-0.30}(syst.)$.

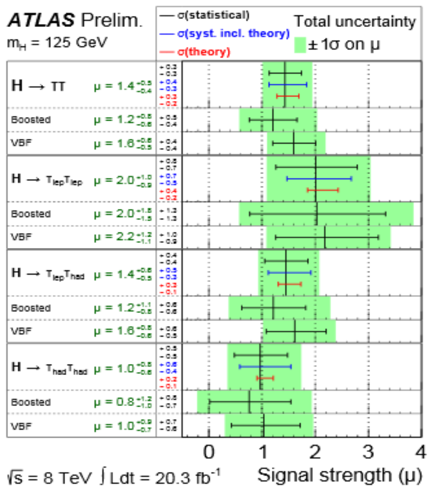

(a) signal strengths for $H \rightarrow \tau\tau$ compared to the SM expectation

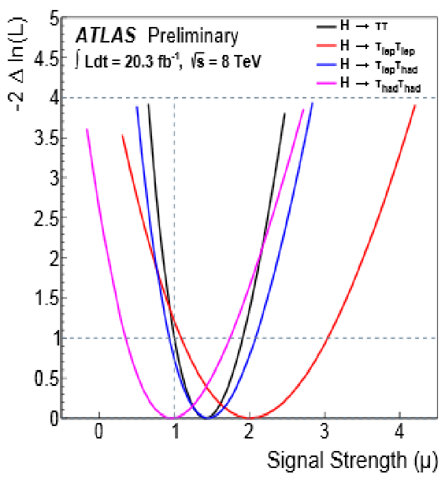

(b) likelihood plot

Figure 23: Results of the ATLAS measurement of $H \rightarrow \tau\tau$ [11]

2.2.2 The CMS measurement of the decay of the 125 GeV Higgs boson into a pair of τ leptons [5]

This search for the $H \to \tau\tau$ decay uses data sets from the CMS experiment at the LHC with integrated luminosities of 4.9 fb^{-1} and 19.7 fb^{-1}, recorded at a centre-off-mass energy of 7 TeV and 8 TeV, respectively.
The events are reconstructed using an particle flow algorithm to combine all information gathered by the CMS subdetectors. Jets are reconstructed from all detected particles with an anti-k_T jet clustering algorithm with a distance parameter of $\Delta R = 0.5$. A jet energy scale correction is performed by using correction factors which depend on the p_T and the η of a jet. Hadronizing b-quarks, which are detected as jets, are reconstructed using a combined secondary vertex (CSV) algorithm. Vertex and shape informations of jets are also used to reject jets originating from pile-up interactions.
Different MC simulation programs, interfaced with a simulation of τ-lepton decays, are used to estimate backgrounds from Z+jets, W+jets, $t\bar{t}$+jets, diboson and single-top production.
Using the SVFIT algorithm, which combines the information of E_T^{miss} with the momenta of the leptons out of the decay of $\tau^+\tau^-$, it is possible to estimate the τ-pair invariant mass more precisely than by just using information from visible decay products (m_{vis}). The achieved resolution is estimated from simulations and is about 10% in the $\tau_h\tau_h$ decay channel, $10-15\%$ in the $l\tau_h$ channel and 20% in the ll' channels, respectively. This gain of resolution is important to improve the separation power of $H \to \tau\tau$ events from the $Z \to \tau\tau$ events, whose contribution as background process is irreducible. The plots in Fig.24 show the reconstructed invariant masses of simulated samples of $H \to \tau\tau$ and $Z \to \tau\tau$ decays from the $\mu\tau_h$ channel.

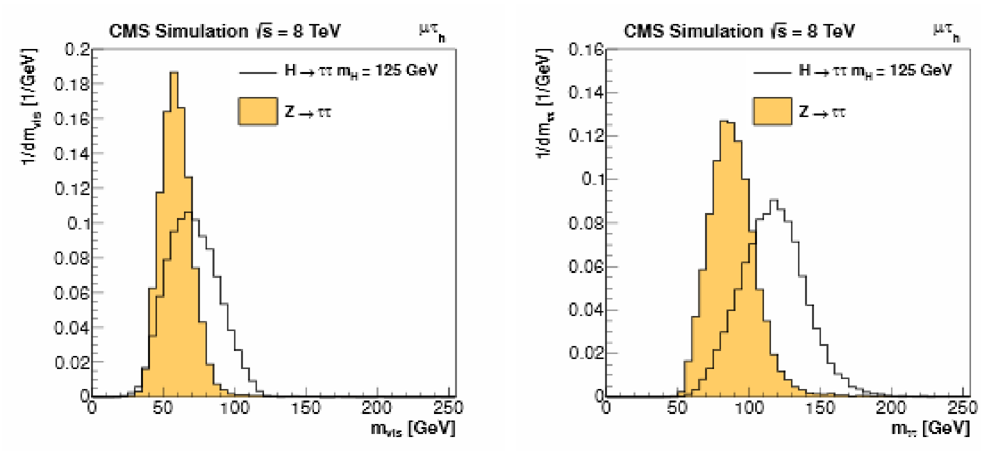

Figure 24: Separation power of the invariant τ-pair mass before (left) and after (right) the application of the SVFIT algorithm in the $\mu\tau_h$ channel [5]

To reduce the background from $t\bar{t}$ processes, a b-tag veto is applied to each analysis

channel. Further cuts and selection criteria are applied to tag the events according to the associated Higgs production mechanism and to minimize background contributions to these tag categories.
For example the Drell-Yan background of $Z \rightarrow \tau\tau$ is greatly reduced in the 1-jet and VBF tag selection, because the jet-multiplicity distribution of Drell-Yan process is decreasing rapidly. The MC modelling of this process uses (as in the search of ATLAS) the "embedding" method, applied on a sample of recorded $Z \rightarrow \mu\mu$ events.
Another important example for the treatment of background processes is the W+jets production with its significant contribution to the $e\tau_h$ and $\mu\tau_h$ channels due to the leptonic decay of the W boson and the misidentification of the jet as τ_h. Here the MC simulations are validated in a high-m_T control region ($m_T > 70GeV$) where the m_T distribution is greatly dominated by electroweak W+jets processes. This is presented in the following Fig.25.

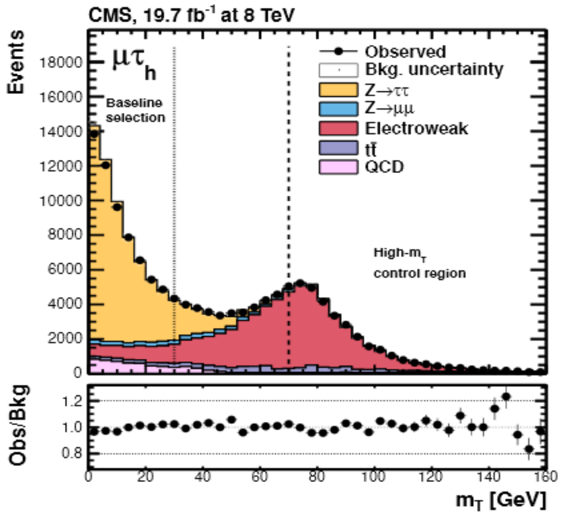

Figure 25: m_T distribution before the general cut $m_T > 30$ TeV is applied. The dashed line illustrates the high-m_T control region for the electroweak background including W+jets, diboson and single-top processes. The bottom inset shows the event yield compared to the SM expectation for each bin. The "Bkg. uncertainty" combines statistical and syststematical uncertainties from each bin. [5]

Due to the small number of signal events in the single channels of the analysis, they are combined to get a joint result. This is done by weighting every category of each channel with the ratio of expected signal to signal-plus-background for the central range of $m_{\tau\tau}$, containing 68% of the signal events. The signal distribution in the plot in Fig.26 is normalized to the SM expectation of $\mu = 1$.

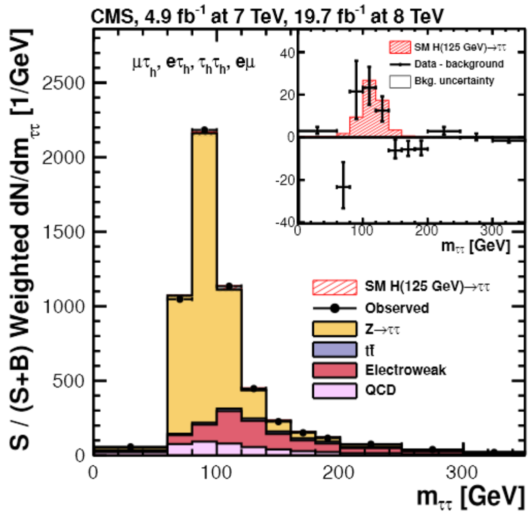

Figure 26: S/(S+B) weighted combined $m_{\tau\tau}$ distribution from the $\mu\tau_h$, $e\tau_h$, $\tau_h\tau_h$ and $e\mu$ channels [5]

The measured signal strengths with respect to the SM expectation are calculated for each channel and each category and combined to an overall best-fit value of $\mu = 0.78 \pm 0.27$ for $m_H = 125GeV$, shown in the following Fig.27.

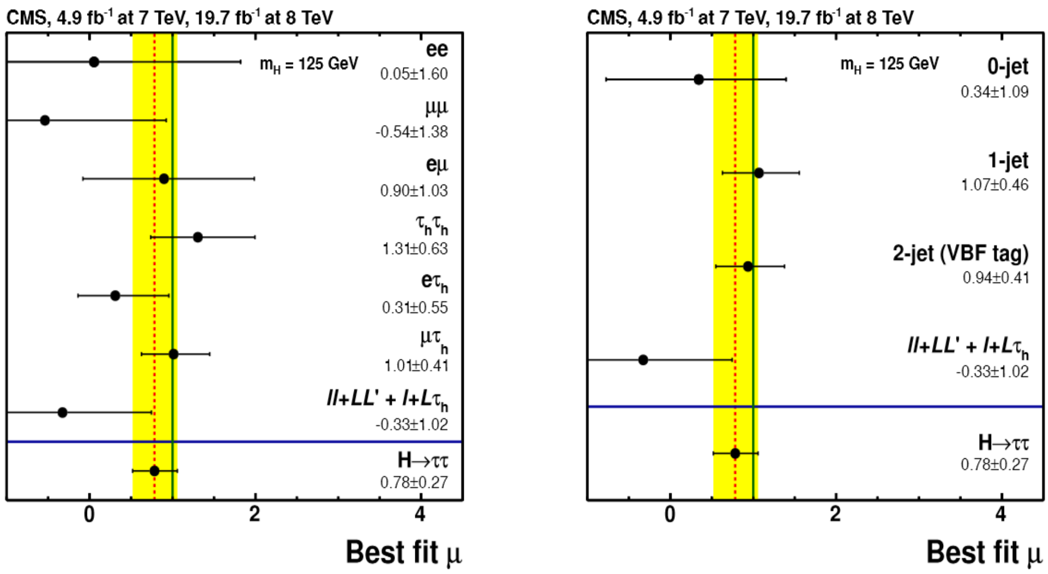

Figure 27: Measured signal strengths with respect to the SM expecation for different decay channels and Higgs production categories [5]

3 Results

3.1 The search $H \rightarrow b\bar{b}$

In this analysis, both experiments used a preselection for the production of a Higgs particle via vector boson associated Higgs production. The subsequent decay into a pair of b-quarks has been investigated.

The ATLAS search for the decay of the Higgs particle into a pair of b-quarks does not report any significance. The measured signal strength is $\mu = 0.2 \pm 0.5(stat.) \pm 0.4(syst.)$, which leaves the question open if there is a SM-like coupling of the Higgs particle to b-quarks.
On the other hand, the CMS search reports an excess of data over the expected background in every analysis channel, which is consistent with $\mu = 1$. The combined value for the signal strength of the coupling $H \rightarrow \tau\tau$ compared to the SM expectation is $\mu = 1.0 \pm 0.5$, which supports the assumption that the SM coupling is realized.

Summarizing the searches, both are consistent with the SM expectation of $\mu = 1$ within their 1σ error intervals. It can be concluded that the decay $H \rightarrow \tau\tau$ is realized in nature and has to be investigated further to exclude smaller discrepancies between the SM and the results of the experiments.

3.2 The search $H \rightarrow \tau\tau$

The decay $H \rightarrow \tau\tau$ is probed for all different Higgs production mechanisms, i.e. gluon fusion, vector boson associated production and vector boson fusion.

The ATLAS experiment measures $H \rightarrow \tau\tau$-couplings which are (almost) consistent with $\mu = 1$ for every single decay mode of a τ pair and combines them to an overall measurement of the signal strength to yield $\mu = 1.43^{+0.31}_{-0.29}(stat.)^{+0.41}_{-0.30}(syst.)$.
CMS confirms this result with a SM consistent measurement of the signal strengths for all different production modes of the Higgs particle and all decay modes of the τ pair from the Higgs decay.
The combined CMS measurement of the signal strength for the coupling in the process $H \rightarrow \tau\tau$ is $\mu = 0.78 \pm 0.27$.

Both measurements of ATLAS and CMS support the SM hypothesis concerning the coupling of the 125 GeV Higgs boson to τ leptons. Futher inverstigations with reduced systematical and statistical uncertainties are now needed to unveil if there are physical effects beyond the expectations of the SM.

4 References

[1] Ivo van Vulpen. *"Lecture Notes: The Standard Model Higgs Boson"*. 2014. URL: http://master.particles.nl/LectureNotes/2011-PPII-Higgs.pdf (visited on 08/26/2014).

[2] Various. *"Yukawa Interaction"*. 2014. URL: http://en.wikipedia.org/wiki/Yukawa_interaction.

[3] Christopher Schwan. *"Final Project: Higgs decay"*. URL: http://www.students.uni-mainz.de/cschwan/higgs-final_project.pdf (visited on 08/26/2014).

[4] Marco Zanetti. *"Prospects for precision Higgs physics with ATLAS and CMS at High Luminosity LHC"*. On behalf of ATLAS and CMS Collaboration. URL: https://indico.cern.ch/event/253774/session/3/contribution/25/material/slides/1.pdf (visited on 08/26/2014).

[5] The CMS Collaboration. "Evidence for the 125 GeV Higgs Boson decaying to a pair of τ leptons". In: *SISSA* (January 20, 2014).

[6] Markus Schumacher & Stan Lai. *"Chapter7: Test of the Electroweak Standard Model, Part 4: Investigations of the new boson"*. Lecture: Hadron Collider Physics, ss14, University of Freiburg. URL: https://terascale.physik.uni-freiburg.de/lehre/ss_14/Vorlesungsfolien/Chapter7Part4 (visited on 08/26/2014).

[7] The ATLAS Collaboration. *"Event Displays of Some Candidate Events Selected in Higgs Search Analyses"*. from: ATLAS Experiment - Public Results. URL: https://twiki.cern.ch/twiki/bin/view/AtlasPublic/EventDisplaysFromHiggsSearches#H_WH_l_bb (visited on 08/26/2014).

[8] The CDF Collaboration. *"Search for Standard Model Higgs Boson Production in Association with a W Boson Using a Matrix Element Technique at CDF in $p\bar{p}$ Collisions at $\sqrt{s} = 1.96$ TeV"*. Phys.Rev. D85 (2012) 072001, DOI: 10.1103/PhysRevD.85.072001. URL: http://inspirehep.net/record/1082043?ln=de (visited on 08/26/2014).

[9] The ATLAS Collaboration. "Search for the $b\bar{b}$ decay of the Standard Model Higgs boson in associated (W/Z)H production with the ATLAS detector". In: *ATLAS-CONF NOTES* (2013).

[10] The CMS Collaboration. "Search for the standard model Higgs boson produced in association with a W or a Z voson and decaying to bottom quarks". In: *Physical Review D **89**, 012003 (2014)* (published 21 January 2014).

[11] The ATLAS Collaboration. "Evidence for Higgs Boson Decays to the $\tau^+\tau^-$ Final State with the ATLAS Detector". In: *ATLAS-CONF NOTES* (28 November 2013).